

Very low sound velocities in iron-rich (Mg,Fe)O: Implications for the core-mantle boundary region

J. K. Wicks,¹ J. M. Jackson,^{1,2} and W. Sturhahn^{3,4}

Received 22 April 2010; revised 9 June 2010; accepted 21 June 2010; published 10 August 2010.

[1] The sound velocities of (Mg₁₆Fe₈₄)O have been measured to 121 GPa at ambient temperature using nuclear resonant inelastic x-ray scattering. The effect of electronic environment of the iron sites on the sound velocities were tracked *in situ* using synchrotron Mössbauer spectroscopy. We found the sound velocities of (Mg₁₆Fe₈₄)O to be much lower than those in other presumed mantle phases at similar conditions, most notably at very high pressures. Conservative estimates of the effect of temperature and dilution on aggregate sound velocities show that only a small amount of iron-rich (Mg,Fe)O can greatly reduce the average sound velocity of an assemblage. We propose that iron-rich (Mg,Fe)O be a source of ultra-low velocity zones. Other properties of this phase, such as enhanced density and dynamic stability, strongly support the presence of iron-rich (Mg,Fe)O in localized patches above the core-mantle boundary. **Citation:** Wicks, J. K., J. M. Jackson, and W. Sturhahn (2010), Very low sound velocities in iron-rich (Mg,Fe)O: Implications for the core-mantle boundary region, *Geophys. Res. Lett.*, 37, L15304, doi:10.1029/2010GL043689.

1. Introduction

[2] The core-mantle boundary (CMB) layer, often called D'', spans up to 350 km of the lower mantle above the liquid outer core, corresponding to a proposed temperature and pressure range of ~3300–4300 K and 115–135 GPa [Garnero and Helmberger, 1995]. Intermittent detection of seismic reflections from the top of D'' suggests that the CMB layer is compositionally heterogeneous and/or represents different phase assemblages [Lay et al., 2008; Sidorin et al., 1999]. Interaction of the CMB layer with the liquid outer core could further augment this heterogeneity, causing it to be enriched in iron. Therefore, large amounts of iron could be considered in the equilibrium assemblages of the CMB.

[3] Seismic observations near the base of the CMB have detected 5–20 km thick patches in which the seismic wave velocities are reduced by up to 30% [Thorne and Garnero, 2004]. These ultra-low velocity zones (ULVZs) have been attributed to a metal-bearing layer [Manga and Jeanloz, 1996], iron-enriched post-perovskite [Mao et al., 2004], and most popularly to partial melting [Williams et al., 1998; Lay et al., 2004; Labrosse et al., 2007; Mosenfelder et al.,

2009]. However, partially molten zones require complex geometry or chemistry to match seismic and dynamic constraints [Rost et al., 2006; Hernlund and Tackley, 2007], and the correct interpretation of seismic signatures requires knowledge of the wave velocities and chemical composition of candidate phases at CMB conditions.

[4] The major phases expected to be in the CMB region are (Mg,Fe)O, and perovskite (Pv)- and/or postperovskite (PPv)-structured silicates. An enhanced iron content and subsequent oxidative uptake by (Mg,Fe)O could result in a iron-rich composition of (Mg,Fe)O distinct from that normally in equilibrium with the rest of the mantle. It has been shown that liquid iron can react with ferrous iron-bearing perovskite to produce perovskite, FeSi, and FeO [Knittle and Jeanloz, 1991; Song and Ahrens, 1994]. Additionally, recent experimental results, based on analyses of quenched phase assemblages from $P \sim 100$ GPa and $T \sim 1800$ K, suggest that iron preferentially partitions into (Mg,Fe)O in the presence of Pv- and PPv-structured silicates [Murakami et al., 2005; Auzende et al., 2008; Sinmyo et al., 2008]. It is therefore timely to study the wave velocities of iron-rich (Mg,Fe)O approaching CMB conditions to test whether this phase is compatible with seismic observations. We present the sound velocities of (Mg₁₆Fe₈₄)O up to 121 GPa and show that iron-rich (Mg,Fe)O is a robust candidate for a compositionally distinct ULVZ.

2. Experiments and Data Evaluation

[5] Three panoramic diamond anvil cells (DACs) were prepared for this experiment. Details of synthesis and purity can be found in auxiliary material.¹ High-pressure nuclear resonance scattering experiments were conducted at Sector 3 of the Advanced Photon Source at Argonne National Laboratory [Sturhahn and Jackson, 2007]. The storage ring was operated in top-up mode with 24 bunches separated by 153 ns. The x-ray energy incident on the sample had a bandwidth of 1.2 meV and was tuned around the 14.4125 keV nuclear resonance of ⁵⁷Fe. Time-delayed photons resulting from nuclear excitation of the ⁵⁷Fe isotope in (Mg₁₆Fe₈₄)O were collected using three avalanche photodiode detectors (APDs) positioned radially around the DAC. At each pressure, inelastically scattered photons were collected over select energy ranges spanning -80 meV to +100 meV. Nuclear resonance inelastic X-ray scattering (NRIXS) spectra were collected from ambient pressure to 121 GPa at 300 K. From the measured energy spectra, the partial phonon density of states (PDOS) pertaining to the Fe site was extracted using previously described methods [Sturhahn and Jackson, 2007] (Figure 1a).

¹Division of Geological and Planetary Sciences, California Institute of Technology, Pasadena, California, USA.

²Seismological Laboratory, California Institute of Technology, Pasadena, California, USA.

³Advanced Photon Source, Argonne National Laboratory, Argonne, Illinois, USA.

⁴Now at Jet Propulsion Laboratory, Pasadena, California, USA.

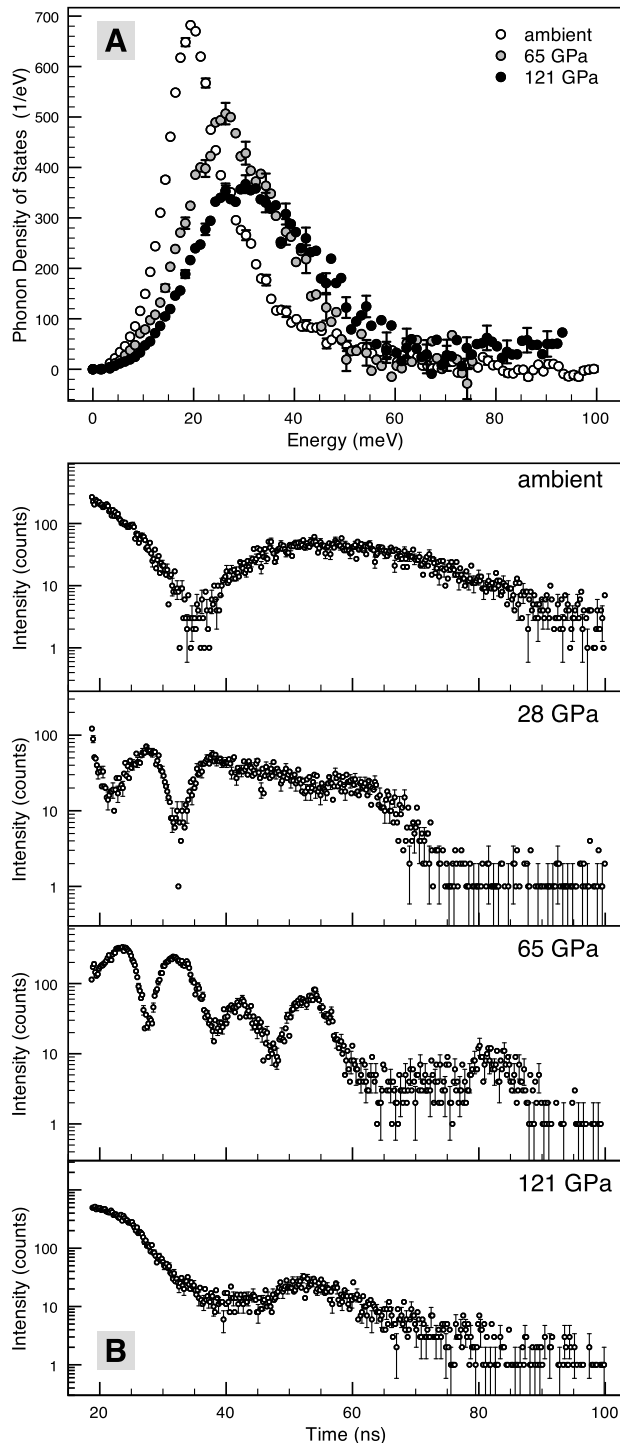


Figure 1. Typical NRS data at 300 K. (a) Partial phonon density of states of (Mg₁₆Fe₈₄)O at select pressures. (b) Time spectra of (Mg₁₆Fe₈₄)O from synchrotron Mössbauer spectroscopy. The ambient pressure spectrum is characterized by slow oscillations, consistent with no magnetic ordering. Fast oscillations appear in the spectrum at 28 GPa. The spectrum at 65 GPa represents a magnetically-ordered state that is stable between 28 and 110 GPa. At 121 GPa, the fast oscillations have disappeared, which is indicative of a spin transition to a low-spin state of the Fe 3d-electron configuration. Error bars are shown for every fourth point.

[6] A fourth APD was positioned in the forward direction with two goals: 1) to measure the resolution function for accurate sound velocity determination and 2) to measure the time spectra using synchrotron Mössbauer spectroscopy for local magnetic environment determination of the ⁵⁷Fe (Figure 1b).

[7] The Debye sound velocity, V_D , is related to the low-energy region of the PDOS in the following manner

$$V(E) = \left\{ \frac{mE^2}{2\pi^2\hbar^3\rho D(E)} \right\}^{\frac{1}{3}} \text{ and } V_D = V(0). \quad (1)$$

Values of $V(E)$ were calculated from the measured PDOS and matched to an empirical function $f(E) = V_D \{1 - (E/E_0)^2\}$, where E_0 and V_D are optimized in a standard least-square-fit procedure [Jackson *et al.*, 2009]. The energy region for the fit was chosen between about 4 and 14 meV. In the auxiliary material, we illustrate the V_D -fitting procedure. In Figure 2a, we plot V_D 's determined for the entire pressure range. For comparison, we also show V_D 's of Fe₉₄₇O that we determined from the PDOS's reported in another NRIXS study, which was conducted at 300 K up to 49 GPa [Struzhkin *et al.*, 2001].

[8] For an isotropic solid, V_D is related to the seismically relevant aggregate compressional (V_P) and shear (V_S) velocities by $3/V_D^3 = (1/V_P^3) + (2/V_S^3)$ and $V_P^2 - (4/3)V_S^2 = K_{0S}/\rho$ [Sturhahn and Jackson, 2007], where K_{0S} is the adiabatic bulk modulus at ambient temperature, ρ is the density, and V_ϕ is the bulk sound velocity. K_{0S} is related to the isothermal bulk modulus, K_{0T} , by $K_{0S} = K_{0T}(1 + \alpha\gamma T)$. K_{0S} can be approximated by K_{0T} , because at room temperature $\alpha\gamma T < 0.01$. The isothermal third order Birch-Murnaghan weighted equation of state (EOS) from a high-pressure powder x-ray diffraction study up to 93 GPa on (Mg₂₂Fe₇₈)O, a similar composition to that used in our NRIXS measurements, provided the values $K_{0T} = 191.2 \pm 5.5$ GPa and $K'_{0T} = 2.5 \pm 0.1$ [Zhuravlev *et al.*, 2009]. The pressure-dependent density of (Mg₁₆Fe₈₄)O was obtained by rescaling this EOS with our initial volume and density. X-ray diffraction spectra of our sample were taken at select pressures, including ambient, at the Advanced Light Source at Lawrence Berkeley National Laboratory, confirming our choice of EOS and pressure scale. The seismically relevant V_P and V_S values determined at each pressure point are shown for the entire pressure range (Figure 2b).

3. Results

[9] At ambient pressure, the velocities of (Mg₁₆Fe₈₄)O are in very good agreement with the trend in sound velocities for iron-rich (Mg,Fe)O [Jacobsen *et al.*, 2002; Struzhkin *et al.*, 2001] (Figure 2b). *In situ* synchrotron Mössbauer spectroscopy shows an absence of magnetic ordering (Figure 1) at low pressures, and detailed analysis reveals a quadrupole splitting of about 0.8 mm/s. At pressures approaching 28 GPa, both V_D and V_S of (Mg₁₆Fe₈₄)O decrease with increasing pressure (Figures 2a and 2b). The softening occurs in the vicinity of the transition from the paramagnetic state to a magnetically ordered state around 28 GPa (Figure 1b). The presence of magnetic hyperfine fields is clear evidence for a magnetically ordered state demonstrating a magnetic transition in (Mg₁₆Fe₈₄)O around 28 GPa at 300 K—a finding in agreement with a conventional Mössbauer study

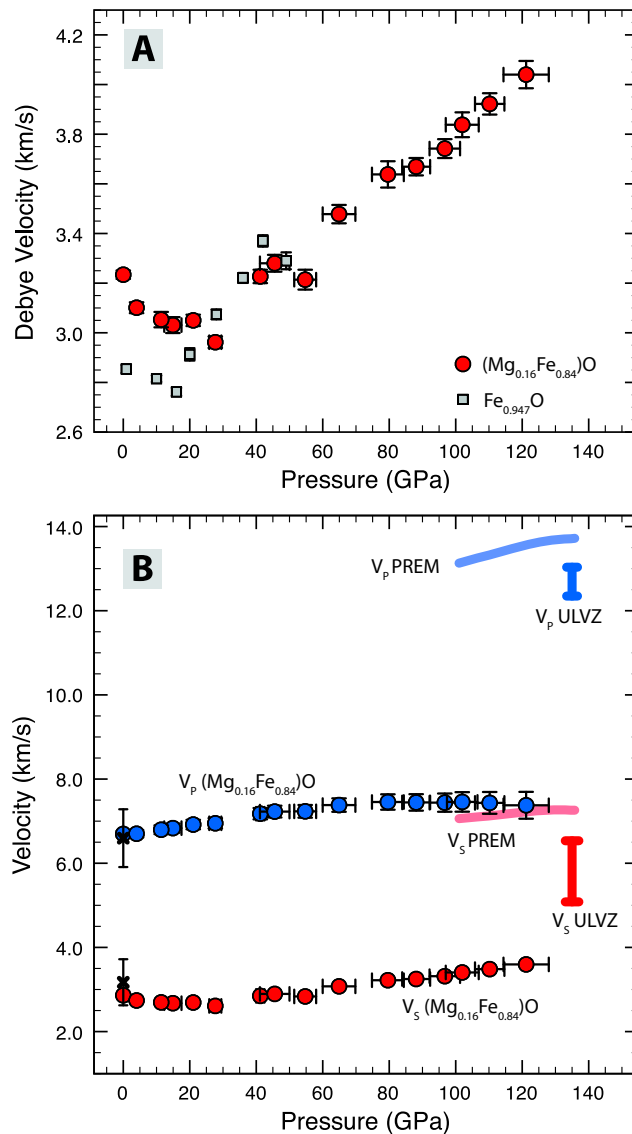


Figure 2. (a) Debye sound velocities determined from the PDOS of (Mg_{0.16}Fe_{0.84})O (this study) and of Fe_{0.947}O [Struzhkin *et al.*, 2001] at 300 K. (b) V_P (red) and V_S (blue), of (Mg_{0.16}Fe_{0.84})O determined from V_D along with PREM and ULVZ's. Crosses: predicted sound velocities for (Mg_{0.16}Fe_{0.84})O from an ultrasonic study [Jacobsen *et al.*, 2002].

on (Mg_{0.20}Fe_{0.80})O [Speziale *et al.*, 2005]. A similar softening is observed for Fe_{0.947}O [Struzhkin *et al.*, 2001](Figure 2a) and other iron-rich (Mg,Fe)O samples [Jacobsen *et al.*, 2004]. This particular behavior has been associated with phonon-magnon coupling [Struzhkin *et al.*, 2001] and may also be related to the B1 to rhombohedral structural distortion.

[10] At 121 GPa the fast oscillations, thus the magnetic hyperfine fields, disappear in the time spectrum (Figure 1b), and is consistent with the onset of a spin transition into a low-spin state of the Fe 3d-electron configuration. We note that at pressures above 100 GPa, V_P ceases to increase and gradually softens. Such a behavior is consistent with a transition to a low spin state, as similar observations have been reported for iron-poor (Mg,Fe)O in the vicinity of a spin transition [Crowhurst *et al.*, 2008]. Most important, the very low pressure derivatives of V_P and V_S for

(Mg_{0.16}Fe_{0.84})O above 28 GPa persist to the highest pressure measured and ensure that this material retains ultra-low sound velocities at core-mantle boundary pressures.

4. Ultra-low Velocity Zones

[11] The shear sound velocity of (Mg_{0.16}Fe_{0.84})O at 121 GPa is about 55% and 50% reduced compared to MgO [Murakami *et al.*, 2009] and the Preliminary Reference Earth Model (PREM) [Dziewonski and Anderson, 1981], respectively. The V_P/V_S ratio at the highest pressure measured is 2.1 ± 0.1 , which falls within the V_P/V_S range of ULVZs (2.2 ± 0.3) [Thorne and Garnero, 2004]. The Poisson ratios (ν) determined from seismic ULVZ observations range from 0.30 to 0.41 and compare favorably to our value of 0.34 ± 0.02 for iron-rich (Mg,Fe)O at 121 GPa and 300 K.

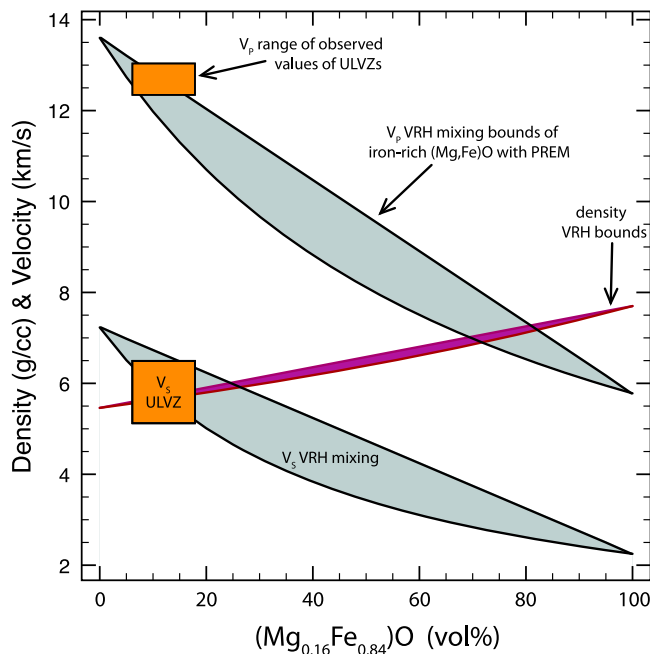


Figure 3. Voigt-Reuss-Hill (VRH) mixing of V_P , V_S , and density (red line) of $(\text{Mg}_{0.16}\text{Fe}_{0.84})\text{O}$ with PREM (see text for details). In orange boxes, we plot V_P and V_S of the ULVZ's centered at 12 vol% $(\text{Mg}_{0.16}\text{Fe}_{0.84})\text{O}$, which produces a v of about 0.34. This particular calculation assumes a pressure of 123 GPa and a temperature of 2700 K. The widths of the ULVZ symbols are arbitrary.

[12] At thousands of K and regardless of its structure [Lin *et al.*, 2003], $(\text{Mg}_{0.16}\text{Fe}_{0.84})\text{O}$ is unlikely to be stiffer than it is at room temperature, which could result in even lower sound velocities at the CMB. As an illustration of the expected V_P , V_S , and density of a mechanical mixture containing iron-rich $(\text{Mg,Fe})\text{O}$ and ambient mantle material, we estimate the effect of temperature on $(\text{Mg}_{0.16}\text{Fe}_{0.84})\text{O}$'s properties using MgO behavior as a proxy [Sinogeikin *et al.*, 2000]. Due to the highly uncertain elastic properties of silicates under CMB conditions, we employ PREM as our bound for the remaining silicate fraction, while recognizing that PREM values may underestimate silicate behavior. We then calculate the Voigt-Reuss-Hill mechanical mixing envelopes for V_P , V_S , and density [Watt *et al.*, 1976] for a given vol% of $(\text{Mg}_{0.16}\text{Fe}_{0.84})\text{O}$ and PREM (Figure 3). To first order, mixing of just 12 vol% of $(\text{Mg}_{0.16}\text{Fe}_{0.84})\text{O}$ with 88 vol% silicates (represented here by PREM) matches signature seismic observations for the ULVZ (Figure 3).

[13] While ULVZ provinces are often considered to be patches of dense partial melt, no measurements exist for the sound velocities of partially molten mantle material at CMB conditions. The connection between ULVZs and partial melting was popularized by the correlation between ULVZ and hot spot locations [Williams *et al.*, 1998]. However, not all ULVZs are related spatially to hot spots. An alternative explanation of several ULVZ observations is a dense, localized solid layer containing some amount of iron-rich $(\text{Mg,Fe})\text{O}$. A solid dense layer would not require the intersection of the local geotherm and solidus of the mantle and can produce low sound speeds independent of partial melting (Figure 3).

[14] This scenario would require a mechanism in which the $(\text{Mg,Fe})\text{O}$ phase becomes enriched in iron in localized areas of the CMB. It has been suggested that extensive iron enrichment could localize in patches in the vicinity of the CMB due to viscosity variations, because liquid iron can be pulled up into the lower mantle on the km scale [Kanda and Stevenson, 2006]. Iron-rich pockets could represent residue of a fractional crystallization of primordial magma ocean [Labrosse *et al.*, 2007]. In representative mantle assemblages with typical amounts of iron, $(\text{Mg,Fe})\text{O}$ has been identified as the preferred iron sink [Auzende *et al.*, 2008; Sinmyo *et al.*, 2008].

[15] Chemical reaction studies between liquid iron and lower mantle perovskite or oxide have produced a wide range of results, leading to interpretations ranging from production of FeSi and FeO [Knittle and Jeanloz, 1991; Song and Ahrens, 1994] to dissolution of oxygen into liquid iron [Takafuji *et al.*, 2005; Frost *et al.*, 2010], respectively. Further investigations exploring the dependence of these reactions on CMB fugacity and chemistry may address these discrepancies, which could be complicated by the possibility of disequilibria. Nevertheless, the low sound velocities of iron-rich $(\text{Mg,Fe})\text{O}$ provide compelling motivation to explore the distribution of iron-rich $(\text{Mg,Fe})\text{O}$ in the core-mantle boundary region.

[16] **Acknowledgments.** We thank H. Yavas, J. Beckett, D. Zhang, C. Murphy, and A. Wolf for assistance with the measurements and NSF-EAR 0711542 and CSEDI EAR-0855815 for financial support. Use of the Advanced Photon Source was supported by the U.S. D.O.E., O.S., O.B.E.S. (DE-AC02-06CH11357). Sector 3 operations are partially supported by COMPRES (NSF EAR 06-49658). The Advanced Light Source is supported by the Director, O.S., O.B.E.S., of the U.S. D.O.E. (DE-AC02-05CH11231). Microprobe analyses were carried out at the Caltech GPS Division Analytical Facility (funded in part by the MRSEC Program of the NSF under DMR-0080065).

References

- Auzende, A. L., J. Badro, F. J. Ryerson, P. K. Weber, S. J. Fallon, A. Addad, J. Siebert, and G. Fiquet (2008), Element partitioning between magnesium silicate perovskite and ferropervicite: New insights into bulk lower-mantle geochemistry, *Earth Planet. Sci. Lett.*, *269*(1–2), 164–174, doi:10.1016/j.epsl.2008.02.001.
- Crowhurst, J. C., J. M. Brown, A. F. Goncharov, and S. D. Jacobsen (2008), Elasticity of $(\text{Mg, Fe})\text{O}$ through the spin transition of iron in the lower mantle, *Science*, *319*(5862), 451–453, doi:10.1126/science.1149606.
- Dziewonski, A. M., and D. L. Anderson (1981), Preliminary reference Earth model, *Phys. Earth Planet. Inter.*, *25*(4), 297–356.
- Frost, D. J., Y. Asahara, D. C. Rubie, N. Miyajima, L. S. Dubrovinsky, C. Holzappel, E. Ohtani, M. Miyahara, and T. Sakai (2010), Partitioning of oxygen between the Earth's mantle and core, *J. Geophys. Res.*, *115*, B02202, doi:10.1029/2009JB006302.
- Gamero, E. J., and D. V. Helmberger (1995), A very slow basal layer underlying large-scale low-velocity anomalies in the lower mantle beneath the Pacific: Evidence from core phases, *Phys. Earth Planet. Inter.*, *91*(1), 161–176, doi:10.1016/0031-9201(95)03039-Y.
- Hernlund, J., and P. Tackley (2007), Some dynamical consequences of partial melting in Earth's deep mantle, *Phys. Earth Planet. Inter.*, *162*(1–2), 149–163, doi:10.1016/j.pepi.2007.04.005.
- Jackson, J. M., E. A. Hamecher, and W. Sturhahn (2009), Nuclear resonant X-ray spectroscopy of $(\text{Mg,Fe})\text{SiO}_3$ orthoenstatites, *Eur. J. Miner.*, *21*(3), 551–560, doi:10.1127/0935-1221/2009/0021-1932.
- Jacobsen, S. D., H.-J. Reichmann, H. A. Spetzler, S. J. Mackwell, J. R. Smyth, R. J. Angel, and C. A. McCammon (2002), Structure and elasticity of single-crystal $(\text{Mg,Fe})\text{O}$ and a new method of generating shear waves for gigahertz ultrasonic interferometry, *J. Geophys. Res.*, *107*(B2), 2037, doi:10.1029/2001JB000490.
- Jacobsen, S. D., H. Spetzler, H. J. Reichmann, and J. R. Smyth (2004), Shear waves in the diamond-anvil cell reveal pressure-induced instability in $(\text{Mg, Fe})\text{O}$, *Proc. Natl. Acad. Sci. U. S. A.*, *101*(16), 5867–5871, doi:10.1073/pnas.0401564101.

- Kanda, R. V. S., and D. J. Stevenson (2006), Suction mechanism for iron entrainment into the lower mantle, *Geophys. Res. Lett.*, **33**, L02310, doi:10.1029/2005GL025009.
- Knittle, E., and R. Jeanloz (1991), Earth's core-mantle boundary—Results of experiments at high pressures and temperatures, *Science*, **251**(5000), 1438–1443, doi:10.1126/science.251.5000.1438.
- Labrosse, S., J. Hernlund, and N. Coltice (2007), A crystallizing dense magma ocean at the base of the Earth's mantle, *Nature*, **450**(7171), 866–869, doi:10.1038/nature06355.
- Lay, T., E. J. Garnero, and Q. Williams (2004), Partial melting in a thermochemical boundary layer at the base of the mantle, *Phys. Earth Planet. Inter.*, **146**(3–4), 441–467, doi:10.1016/j.pepi.2004.04.004.
- Lay, T., J. Hernlund, and B. A. Buffett (2008), Core-mantle boundary heat flow, *Nat. Geosci.*, **1**, 25–32, doi:10.1038/ngeo.2007.44.
- Lin, J. F., D. L. Heinz, H. Mao, R. J. Hemley, J. M. Devine, J. Li, and G. Shen (2003), Stability of magnesiowüstite in Earth's lower mantle, *Proc. Natl. Acad. Sci. U. S. A.*, **100**(8), 4405–4408, doi:10.1073/pnas.252782399.
- Manga, M., and R. Jeanloz (1996), Implications of a metal-bearing chemical boundary layer in D'' for mantle dynamics, *Geophys. Res. Lett.*, **23**(22), 3091–3094, doi:10.1029/96GL03021.
- Mao, W. L., G. Shen, V. B. Prakapenka, Y. Meng, A. J. Campbell, D. L. Heinz, J. Shu, R. J. Hemley, and H. Mao (2004), Ferromagnesian post-perovskite silicates in the D'' layer of the Earth, *Proc. Natl. Acad. Sci. U. S. A.*, **101**(45), 15,867–15,869, doi:10.1073/pnas.0407135101.
- Mosenfelder, J. L., P. D. Asimow, D. J. Frost, D. C. Rubie, and T. J. Ahrens (2009), The MgSiO₃ system at high pressure: Thermodynamic properties of perovskite, postperovskite, and melt from global inversion of shock and static compression data, *J. Geophys. Res.*, **114**, B01203, doi:10.1029/2008JB005900.
- Murakami, M., K. Hirose, N. Sata, and Y. Ohishi (2005), Post-perovskite phase transition and mineral chemistry in the pyrolytic lowermost mantle, *Geophys. Res. Lett.*, **32**, L03304, doi:10.1029/2004GL021956.
- Murakami, M., Y. Ohishi, N. Hirao, and K. Hirose (2009), Elasticity of MgO to 130 GPa: Implications for lower mantle mineralogy, *Earth Planet. Sci. Lett.*, **277**(1–2), 123–129, doi:10.1016/j.epsl.2008.10.010.
- Rost, S., E. J. Garnero, and Q. Williams (2006), Fine-scale ultralow-velocity zone structure from high-frequency seismic array data, *J. Geophys. Res.*, **111**, B09310, doi:10.1029/2005JB004088.
- Sidorin, I., M. Gurnis, and D. V. Helmberger (1999), Evidence for a ubiquitous seismic discontinuity at the base of the mantle, *Science*, **286**(5443), 1326–1331, doi:10.1126/science.286.5443.1326.
- Sinmyo, R., K. Hirose, D. Nishio-Hamane, Y. Seto, K. Fujino, N. Sata, and Y. Ohishi (2008), Partitioning of iron between perovskite/postperovskite and ferropericline in the lower mantle, *J. Geophys. Res.*, **113**, B11204, doi:10.1029/2008JB005730.
- Sinogeikin, S. V., J. M. Jackson, B. O'Neill, J. W. Palko, and J. D. Bass (2000), Compact high-temperature cell for Brillouin scattering measurements, *Rev. Sci. Instrum.*, **71**, 201–206, doi:10.1063/1.1150183.
- Song, X., and T. J. Ahrens (1994), Pressure-temperature range of reactions between liquid iron in the outer core and mantle silicates, *Geophys. Res. Lett.*, **21**(2), 153–156, doi:10.1029/93GL03262.
- Speziale, S., A. Milner, V. E. Lee, S. M. Clark, M. P. Pasternak, and R. Jeanloz (2005), Iron spin transition in Earth's mantle, *Proc. Natl. Acad. Sci. U. S. A.*, **102**(50), 17,918–17,922, doi:10.1073/pnas.0508919102.
- Struzhkin, V. V., et al. (2001), Nuclear inelastic X-ray scattering of FeO to 48 GPa, *Phys. Rev. Lett.*, **87**(25), 255501, doi:10.1103/PhysRevLett.87.255501.
- Sturhahn, W., and J. M. Jackson (2007), Geophysical applications of nuclear resonant spectroscopy, in *Advances in High-Pressure Mineralogy*, edited by E. Ohtani, *Spec. Pap. Geol. Soc. Am.*, **421**, 157–174, doi:10.1130/2007.2421(09).
- Takafuji, N., K. Hirose, M. Mitome, and Y. Bando (2005), Solubilities of O and Si in liquid iron in equilibrium with (Mg,Fe)SiO₃ perovskite and the light elements in the core, *Geophys. Res. Lett.*, **32**, L06313, doi:10.1029/2005GL022773.
- Thorne, M. S., and E. J. Garnero (2004), Inferences on ultralow-velocity zone structure from a global analysis of SPdKS waves, *J. Geophys. Res.*, **109**, B08301, doi:10.1029/2004JB003010.
- Watt, J. P., G. F. Davies, and R. J. O'Connell (1976), The elastic properties of composite materials, *Rev. Geophys.*, **14**(4), 541–563, doi:10.1029/RG014i004p00541.
- Williams, Q., J. Revenaugh, and E. Garnero (1998), A correlation between ultra-low basal velocities in the mantle and hot spots, *Science*, **281**(5376), 546–549, doi:10.1126/science.281.5376.54.
- Zhuravlev, K. K., J. M. Jackson, A. S. Wolf, J. K. Wicks, J. Yan, and S. M. Clark (2009), Isothermal compression behavior of (Mg,Fe)O using neon as a pressure medium, *Phys. Chem. Miner.*, **37**, 465–474, doi:10.1007/s00269-009-0347-6.

J. M. Jackson, Seismological Laboratory, Division of Geological and Planetary Sciences, California Institute of Technology, MC 252-21, Pasadena, CA 91125, USA.

W. Sturhahn, Jet Propulsion Laboratory, 4800 Oak Grove Dr., Pasadena, CA 91109, USA.

J. K. Wicks, Division of Geological and Planetary Sciences, California Institute of Technology, MC 170-25, Pasadena, CA 91125, USA. (wicks@gps.caltech.edu)